CHAPTER IV
RESULTS AND DISCUSSION

In this work, the porous media - hollow silica and activated carbon - were selected to study their effects on the methane hydrate formation and dissociation. The methane hydrate experiments were conducted at 6 MPa and 8 MPa and 4°C. The dissociation experiments were observed after the completion of gas hydrate formation experiments. The thermal stimulation method was used in this research to dissociate gas hydrate. In this case, the pressure in the system was decreased from 6 MPa and 8 MPa to 5 MPa and 6.5 MPa, respectively, and the temperature was increased to 25°C. When the temperature crosses the hydrate phase boundary, the hydrate would dissociate, and methane gas would release.

4.1 Effects of Activated Carbon

4.1.1 Methane Hydrate Formation

Table 4.1 presents the methane hydrate formation experimental conditions with the presence of activated carbon at 4°C. The induction time of methane hydrate formation at 8 MPa is close to the methane hydrate formation at 6 MPa, meaning that the methane gas is consumed to form the first hydrate crystal in the same periods of time at the different experimental pressure. Moreover, the methane hydrate in the system of $AC/H_2O/CH_4$ at 6 MPa takes a longer time to reach the equilibrium pressure than the system at 8 MPa. The experimental pressure does not only affect to the time of methane hydrate formation with activated carbon but also the final water conversion to hydrate. The final water conversion to hydrate at 8 MPa is higher than that at 6 MPa. The system with the activated carbon at higher experimental pressure takes less time and shows a higher water conversion to hydrate. Hence, the experimental pressure is one of the gas hydrate driving forces and affects to the kinetics of methane hydrate formation.

Table 4.1 Methane hydrate formation experimental conditions with the presence of activated carbon at 4°C

Exp. No.	System	Experimental Pressure [MPa]	*Induction Time [min]	End of Experiment		Water Conversion to Hydrate [mol%]
				Time [h]	CH_4 Consumed [mol/mol of H_2O]	
1	$AC/H_2O/CH_4$	8	0.17	19	0.1535	93.62
2	$AC/H_2O/CH_4$	8	0.17	36	0.1497	91.31
3	$AC/H_2O/CH_4$	8	0.67	41	0.1484	90.51
				Average	0.1505±0.0026	91.81±1.61
4	$AC/H_2O/CH_4$	6	0.17	34	0.1326	80.85
5	$AC/H_2O/CH_4$	6	0.33	48	0.1320	80.53
6	$AC/H_2O/CH_4$	6	1.67	22	0.1363	83.13
				Average	0.1336±0.0023	81.50±1.42

*Induction Time = time at the first hydrate formation

The formation of gas hydrate is an exothermic process, so it can be noticed by the increase in the temperature, while the pressure in the system is consumed to form the hydrate. Figure 4.1 shows the gas uptake and temperature profiles during the methane hydrate formation of the $AC/H_2O/CH_4$ system at 8 MPa and 4°C (Experiment 3, Table 4.1). The gas uptake in the system of $AC/H_2O/CH_4$ at 8 MPa is rapidly increased after methane gas is introduced into the system, which confirms that the methane hydrate formation occurs very fast at 8 MPa. Initially, the amount of gas uptake increases because of the dissolution of methane gas to water until it saturates (Sun *et al.*, 2008). Then, the rate of gas uptake suddenly increases due to the methane gas is consumed to form the hydrate crystal. The temperatures of all thermocouples rise abruptly at the same time referring to the hydrate formation in different locations at almost the same time. The gas uptake continues to increase until it reaches the limit of hydrate formation.

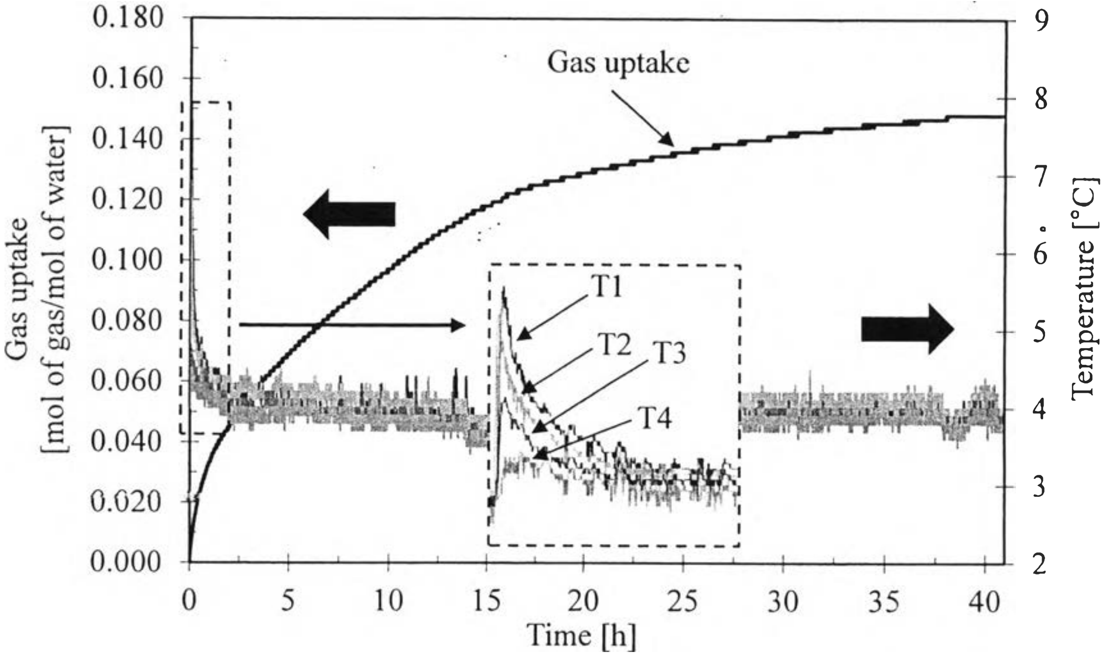

Figure 4.1 Gas uptake and temperature profiles during the methane hydrate formation of the AC/H_2O/CH_4 system at 8 MPa and 4°C (Experiment 3, Table 4.1).

The gas uptake and temperature profiles during the methane hydrate formation of the AC/H_2O/CH_4 system at 6 MPa and 4°C (Experiment 4, Table 4.1) is shown in Figure 4.2. As seen from the figure, similar to the system conducted at 8 MPa, the methane hydrate occurs rapidly after methane gas is introduced so the dissolution of gas into water is not observed before the methane hydrate formation. The methane hydrate growth in the system of AC/H_2O/CH_4 at 6 MPa can be divided into two steps. In the first step, the gas uptake increases rapidly because the methane hydrate nucleation is formed and grows at the interface between water and methane. In the second step, the slope of gas uptake increases again because the methane hydrate at the interface may crack, and water molecules from the cracked hydrated would form the methane hydrate again (Jin *et al.*, 2012). The increased temperature in the second step is not as obvious as the first step because the temperature in system is proportional to the extent of methane hydrate and heat transfer effects (Babu *et al.*, 2013b). It can be indicated that the methane hydrate, formed in the second step has lower extent than that in the first step so the heat released from the methane hydrate formation was lower and easier to transfer than the first step. Thus, the second step of the methane hydrate formation not shows significant spikes in temperature profiles.

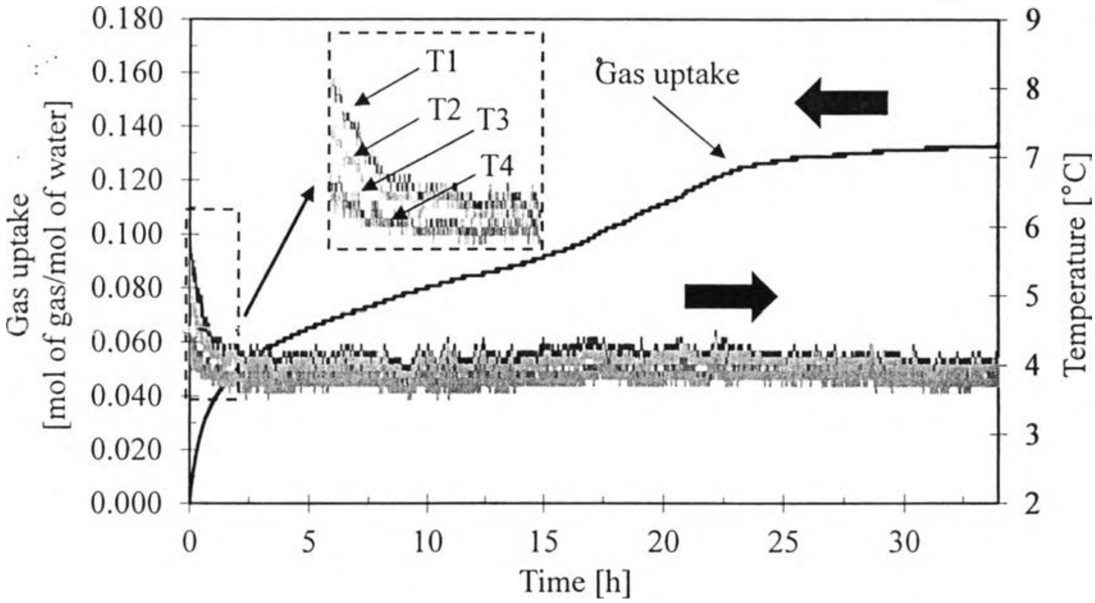

Figure 4.2 Gas uptake and temperature profiles during the methane hydrate formation of the $AC/H_2O/CH_4$ system at 6 MPa and 4°C (Experiment 4, Table 4.1).

The methane hydrate formation in porous media was reported by Babu *et al.* (2013a) and Chari *et al.* (2013). They concluded that the methane hydrate formation is more favorable at the center of pore spaces than at grain surface, and the rate of gas hydrate formation and hydrate growth depended on mass transfer of methane gas into water. Thus, the numerous pores and interstices of activated carbon increase the contact area between methane gas and water, resulting in the increase in the mass transfer of gas into water. However, the methane hydrate formation may cover surface and pores of activated carbon so the rate of methane hydrate and hydrate growth is decreased (Kang and Lee., 2010).

The rates of gas uptake during the methane hydrate formation at 8 MPa and 6 MPa are compared in Figure 4.3. The two steps of methane hydrate formation can be observed in the system of $AC/H_2O/CH_4$ conducted at 6 MPa, while the hydrate growth in the system at 8 MPa is only one step. The hydrate growth in the system of $AC/H_2O/CH_4$ at 8 MPa is significantly higher than the system at 6 MPa because the pressure driving force effects to the rate of hydrate formation with the presence of the activated carbon.

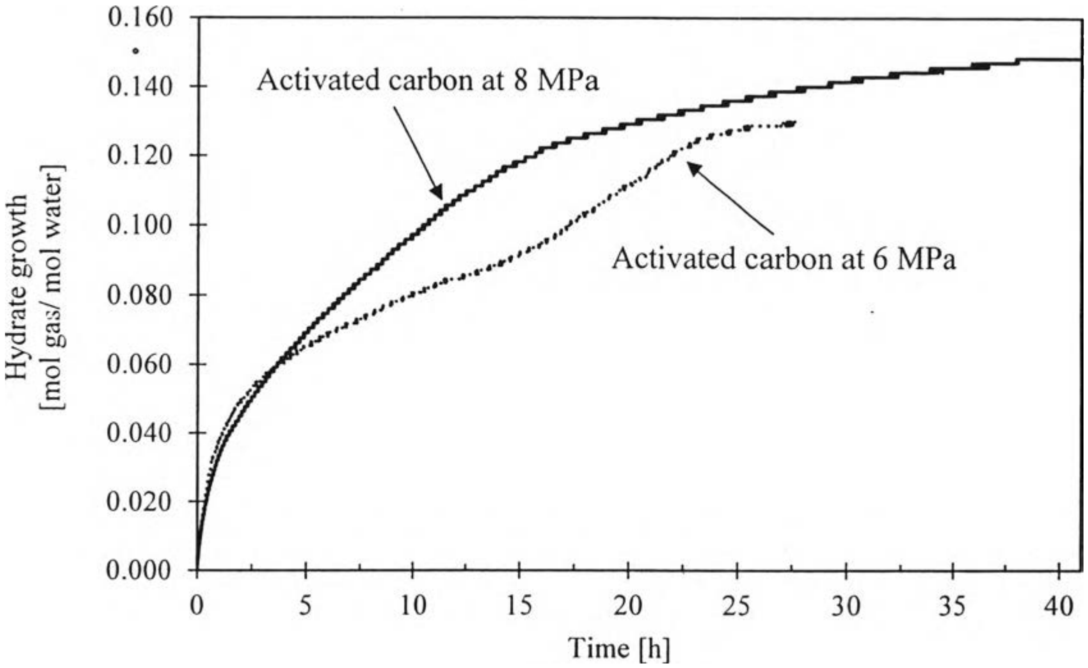

Figure 4.3 Comparison of hydrate growth during the methane hydrate formation in the system of AC/H_2O/CH_4 at 8 MPa and 6 MPa at 4°C (Experiments 3 and 4, respectively, Table 4.1). Time zero in the figure corresponds to the first point of hydrate growth.

4.1.2 Methane Hydrate Dissociation

Table 4.2 presents the methane hydrate dissociation experimental conditions in the system of AC/H_2O/CH_4 at 21°C driving force. The dissociation temperature (T_d) is the first temperature that the methane gas releases from the hydrate form. The dissociation temperature of the system at 6.5 MPa is similar to the system at 5 MPa. It can imply that the methane hydrate starts to dissociate at a higher temperature in the system with the higher experimental pressure. The final methane gas recovery in the system at 6.5 MPa is similar to the system at 5 MPa. The result shows that the experimental pressure does not affect the final methane recovery in the activated carbon system. The system with a higher experimental pressure has higher dissolution of gas into water so, after methane hydrate dissociation, some of methane gas still remains in the water, and it is not recovered (Linga *et al.*, 2009).

Table 4.2 Methane hydrate dissociation experimental conditions in the system with activated carbon with 21°C driving force

Exp. No.	System	Experimental Pressure [MPa]	ΔT^a [°C]	Dissociation Temperature, $T_d{}^b$[°C]	CH_4 Released [mol/mol of H_2O]	CH_4 Recovery [mol%]
1	$AC/H_2O/CH_4$	6.5	21	7.1	0.1058	68.89
2	$AC/H_2O/CH_4$	6.5	21	6.9	0.0949	63.35
3	$AC/H_2O/CH_4$	6.5	21	7.9	0.1025	69.05
				Average	0.1010±0.0056	67.10±3.25
4	$AC/H_2O/CH_4$	5	21	5.6	0.0902	68.03
5	$AC/H_2O/CH_4$	5	21	5.7	0.0953	64.55
6	$AC/H_2O/CH_4$	5	21	5.5	0.0900	66.05
				Average	0.0918±0.0030	66.21±1.75

$^a\Delta T = T_{end} - T_{start}$

^bT_d = Dissociation temperature

Figures 4.4 and 4.5 present the methane released and temperature profiles in the system of $AC/H_2O/CH_4$ at 6.5 MPa and 5 MPa, respectively. After the completion of methane hydrate formation, the temperature in the crystallizer is increased from 4°C to 25°C (temperature driving force = 21°C). The temperature in each thermocouple gradually increases with the water temperature. When the temperature in the crystallizer crosses the hydrate phase equilibrium, the methane hydrate dissociates. At this point, the temperature is called dissociation temperature (T_d), which represents the point on methane hydrate equilibrium curve, as seen in Figures 4.4 and 4.5. At the dissociation temperature, the temperatures in the crystallizer are stabilized between the endothermic process of the hydrate dissociation and the temperature in water bath until the methane hydrate dissociation is completed.

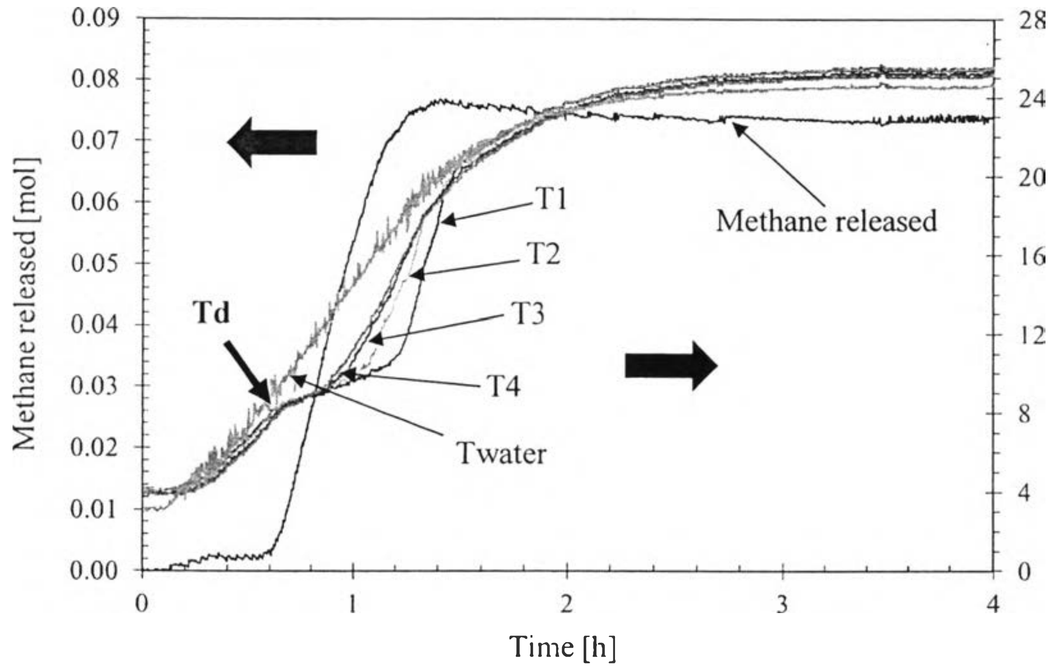

Figure 4.4 Methane released and temperature profiles in the system of AC/H_2O/CH_4 at 6.5 MPa, and temperature driving force = 21°C (Experiment 3, Table 4.2).

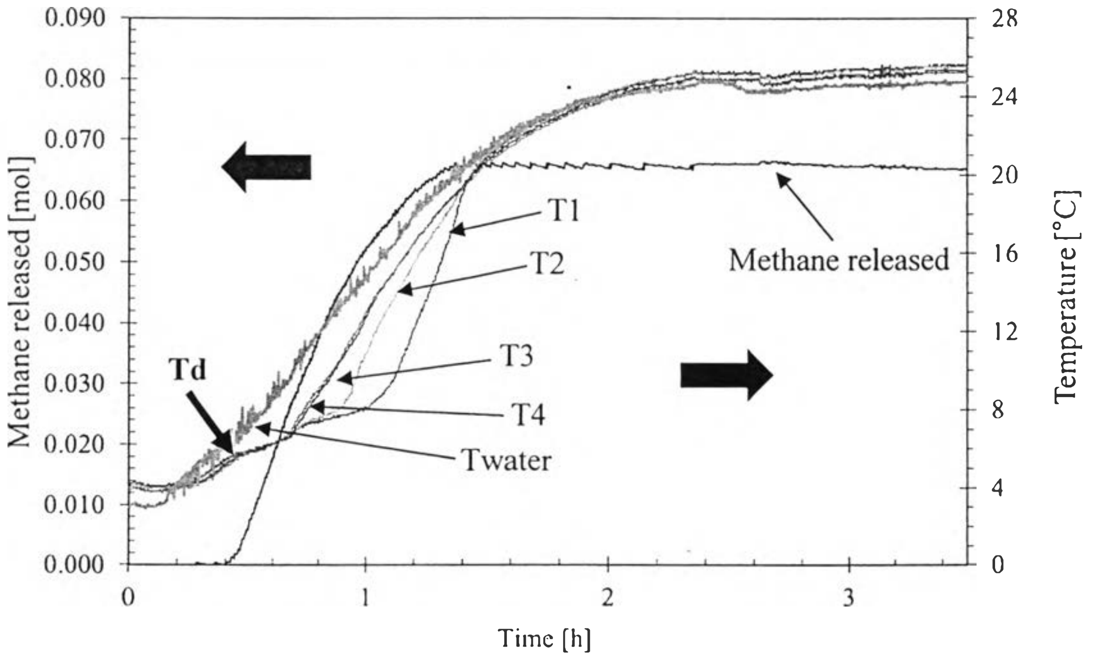

Figure 4.5 Methane released and temperature profiles in the system of AC/H_2O/CH_4 at 5 MPa, and temperature driving force = 21°C (Experiment 4, Table 4.2).

The comparison of the methane released during the methane hydrate dissociation in the system of AC/H_2O/CH_4 at 6.5 MPa and 5 MPa at 4°C is shown in Figure 4.6. The rate of methane released in the system at 6.5 MPa is faster than that at 5 MPa. The amount of methane released in the system with experimental pressure of 5 MPa is slightly lower than that of 6.5 MPa because the system with the experimental pressure of 5 MPa, which is dissociated from 6 MPa has lower amount of gas uptake than that 6.5 MPa. However, the methane released in the system at 6.5 MPa is not significantly different from the system at 5 MPa. Therefore, at the same temperature driving force (21°C), the experimental pressure does not affect the amount of methane released and the final methane recovery but it affects the dissociation rate of methane hydrate, as shown in Figure 4.6.

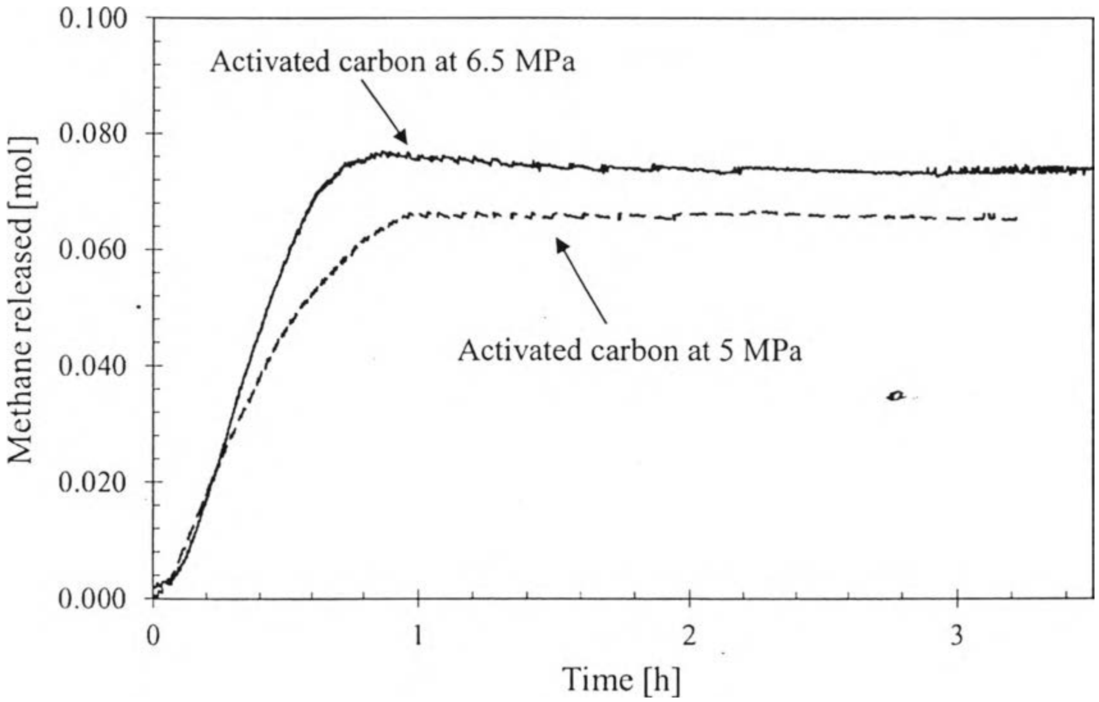

Figure 4.6 Comparison of gas release during the methane hydrate dissociation in the system of AC/H_2O/CH_4 at 6.5 MPa and 5 MPa and temperature driving force = 21°C (Experiment 3 and 4, respectively, Table 4.2). Time zero in the figure corresponds to the first point of hydrate released.

4.2 Effects of Hollow Silica

4.2.1 Methane Hydrate Formation

Table 4.3 presents methane hydrate formation experimental conditions in the system of $HS/H_2O/CH_4$ at 4°C. As seen from the table, the induction time of the $HS/H_2O/CH_4$ system at 6 MPa takes longer time than that at 8 MPa. This result shows the same trend as the system of $AC/H_2O/CH_4$. However, the hydrate formation time and the final water conversion to hydrate at 8 MPa and 6 MPa are about the same. In this case, the methane hydrate conversion is not proportional to the experimental pressure with the presence of hollow silica.

Table 4.3 Methane hydrate formation experimental conditions in the system with hollow silica at 4°C

Exp. No.	System	Experimental Pressure [MPa]	*Induction Time [min]	End of Experiment		Water Conversion to Hydrate [mol%]
				Time [h]	CH_4 Consumed [mol/mol of H_2O]	
7	$HS/H_2O/CH_4$	8	6	15	0.1588	94.32
8	$HS/H_2O/CH_4$	8	3	9	0.1681	99.87
9	$HS/H_2O/CH_4$	8	0.17	6	0.1518	90.19
				Average	0.1596±0.0082	94.79±4.86
10	$HS/H_2O/CH_4$	6	14	12	0.1471	87.38
11	$HS/H_2O/CH_4$	6	0.17	12	0.1420	84.37
12	$HS/H_2O/CH_4$	6	16	12	0.1579	93.78
				Average	0.1490±0.0081	88.51±4.81

*Induction Time = time at the first hydrate formation

Figure 4.7 shows the gas uptake and temperature profiles during the methane hydrate formation of the $HS/H_2O/CH_4$ system at 8 MPa and 4°C. The temperature in the crystallizer with hollow silica rises at T1 first, while the amount of gas uptake increases rapidly. It can be noted that the hydrate formation takes place at the top of crystallizer first and grows to other locations. The multiple temperature spikes indicate the methane hydrate formation at different times and locations, called multiple nucleations (Babu *et al.*, 2013b; Prasad *et al.*, 2012). After that, the amount of gas uptake gradually increases and reaches the plateau, meaning that there is no further hydrate formation in the crystallizer. It can be noted that the hydrate randomly forms in the hollow silica bed because the thermocouples detect the temperature in different locations in the crystallizer. The gas uptake and temperature profiles during the methane hydrate formation of the HS/H_2O/CH_4 system at 6 MPa and 4°C is presented in Figure 4.8. The methane hydrate is randomly formed in hollow silica bed, but overall temperatures in the system at 6 MPa is lower than that at 8 MPa.

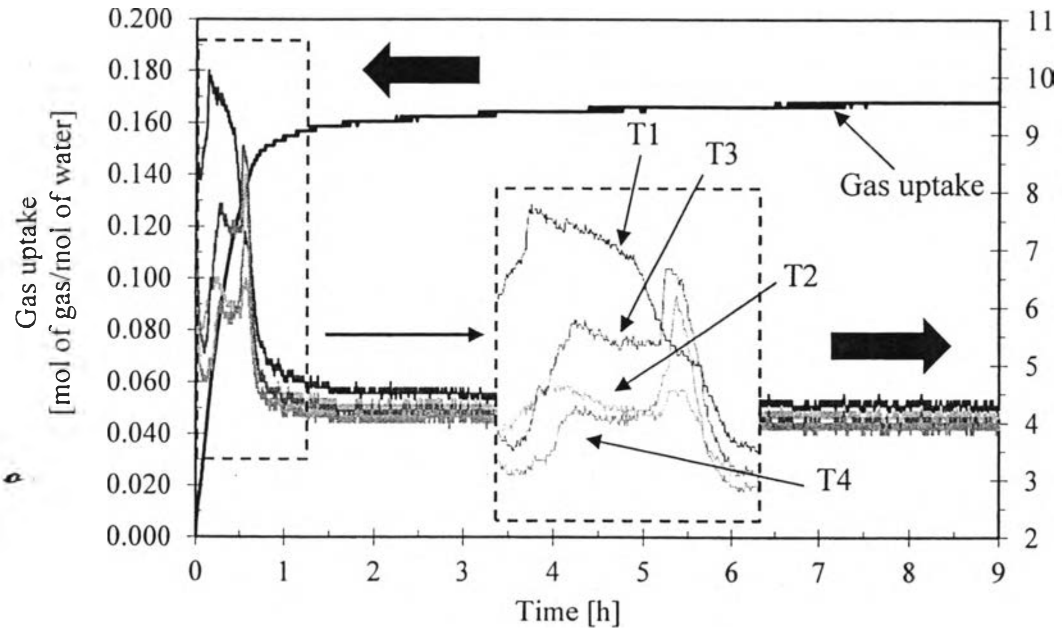

Figure 4.7 Gas uptake and temperature profiles during the methane hydrate formation of HS/H_2O/CH_4 system at 8 MPa and 4°C (Experiment 8, Table 4.3).

I28368865

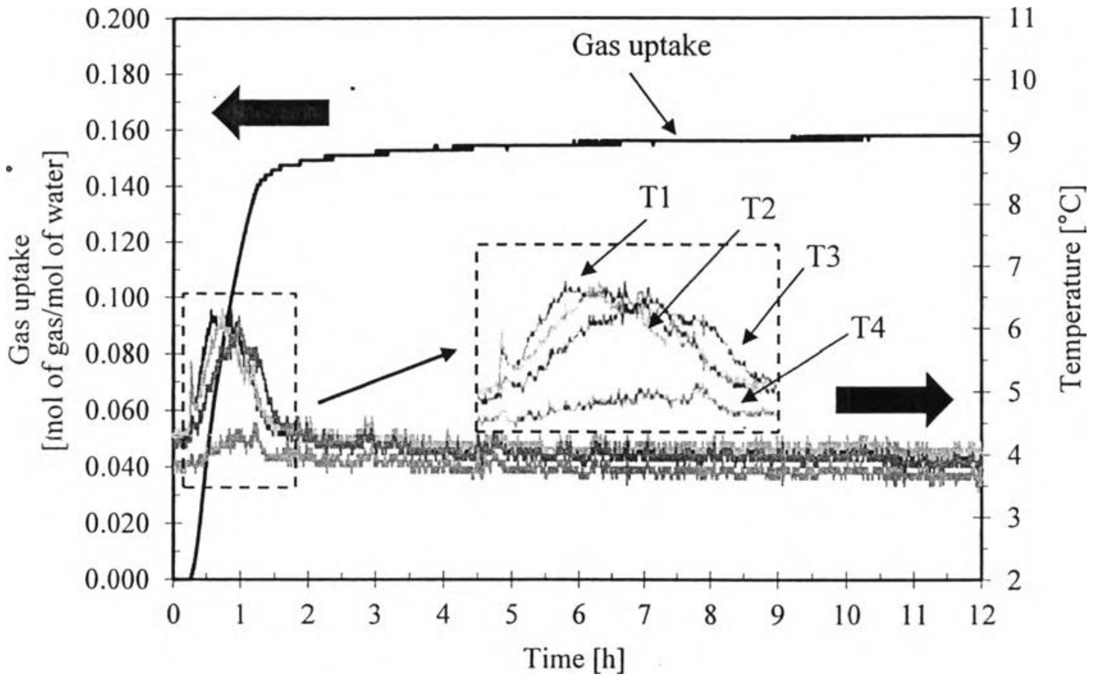

Figure 4.8 Gas uptake and temperature profiles during the methane hydrate formation of $HS/H_2O/CH_4$ system at 8 MPa and 4°C (Experiment 12, Table 4.3).

Figure 4.9 presents the morphology of hollow silica by scanning electron microscope (SEM). The results show that the hollow silica has a smooth surface and round shape like ball in various sizes (diameter 30-70 μm). Some breakage hollow silica show the cavity inside the hollow silica. These cavities are confirmed by transmission electron microscope (TEM), which is shown in Figure 4.10. The cavity insides the hollow silica (brighter area) is covered with a thin wall (darker area) in the same thickness. The hydrate formation is similar to the crystallization process, and the rate of gas hydrate formation and hydrate growth depend on the mass transfer of methane gas to water. The small size of hollow silica powder is highly dispersed in the water phase so it may act as a nucleating agent that can improve the hydrate formation rate and amount of methane consumption (Chari *et al.*, 2013; Prasad *et al.*, 2014).

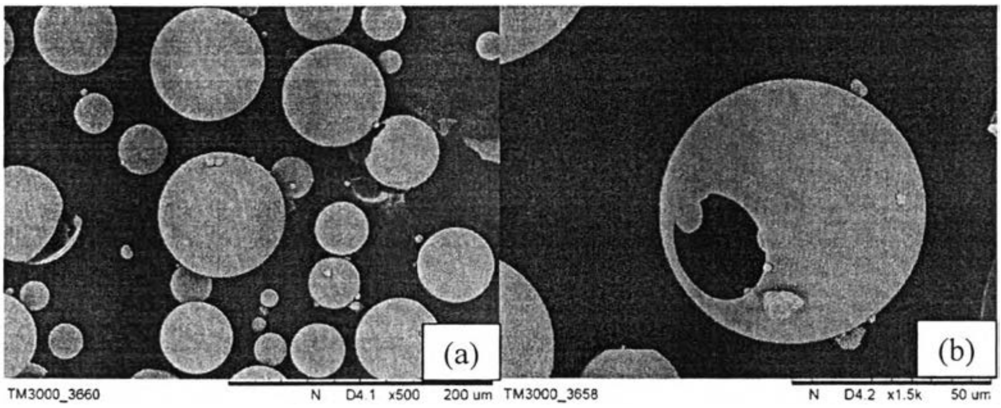

Figure 4.9 Morphology of hollow silica by scanning electron microscope (SEM) (a) Particle of hollow silica in different sizes, (b) Breakage hollow silica.

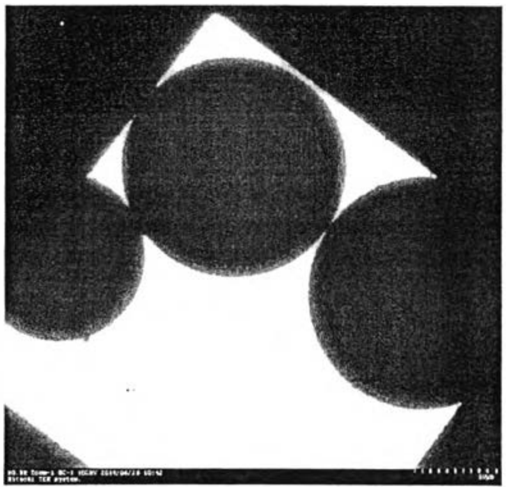

Figure 4.10 Particles of hollow silica by transmission electron microscope (TEM).

Figure 4.11 presents the comparison of gas uptake during the methane hydrate formation in the system of HS/H_2O/CH_4 at 8 MPa and 6 MPa and 4°C. The gas uptake profiles in both systems are almost the same. In other words, the gas uptake is increased rapidly, while the methane hydrate is formed. The rate of gas uptake does not change much after the experimental hydrate starts forming until the gas uptake reaches plateau. Thus, the presence of hollow silica does not affect the rate of the hydrate growth in both conditions (6 and 8 MPa). The induction time in the system at 6 MPa takes longer than the system with the experimental pressure of 8

MPa. But, the rate of hydrate growth, represented by the slope in Figure 4.11, is not significantly different. Hence, the experimental pressure does not affect the rate of methane hydrate formation, which was reported by Chari *et al.* (2013). They concluded that the rate of gas hydrate formation may not always be proportional to the experimental pressure in the system.

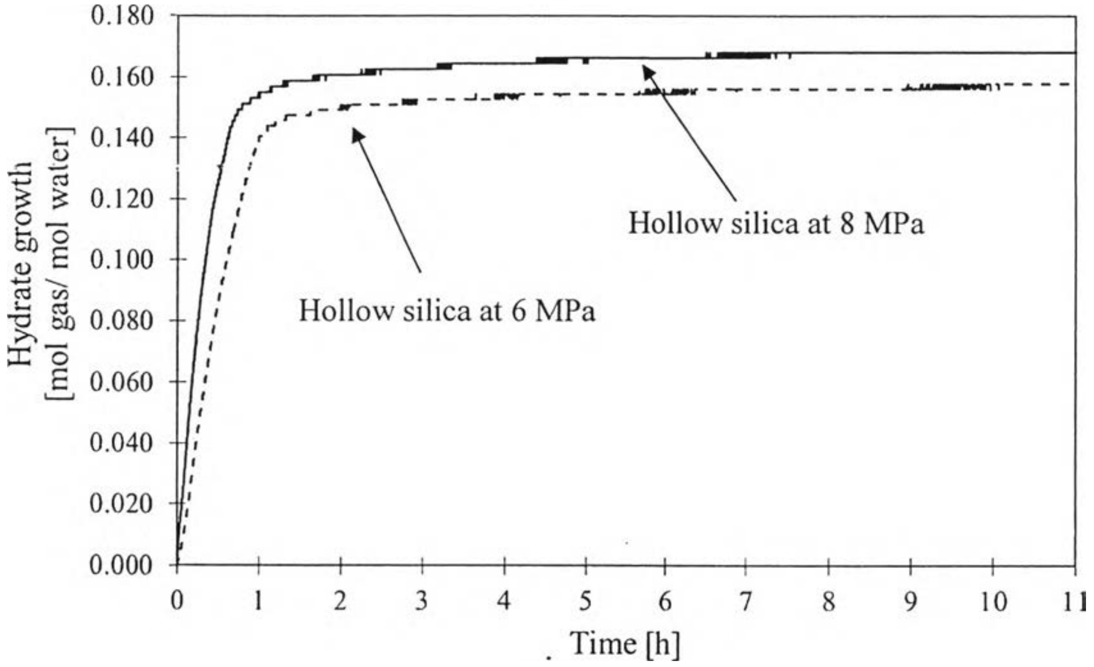

Figure 4.11 Comparison of hydrate growth during the methane hydrate formation in the system of HS/H_2O/CH_4 at 8 MPa and 6 MPa and 4°C (Experiments 8 and 12, respectively, Table 4.3). Time zero in the figured corresponds to the first point of hydrate growth.

4.2.2 Methane Hydrate Dissociation

Table 4.4 shows methane hydrate dissociation experimental conditions in the system of HS/H_2O/CH_4 at 21°C driving force. The final methane recovery in the system at 6.5 MPa and 5 MPa are not significantly different. Hence, the experimental pressure is not proportional to the final methane gas recovery in the case of hollow silica system. The dissociation temperature in the system of HS/H_2O/CH_4 shows similar trend as the system of AC/H_2O/CH_4. In other words, the dissociation temperature in the system at 6.5 MPa is higher than the system at experimental pressure 5 MPa.

Table 4.4 Methane hydrate dissociation experimental conditions in the system with hollow silica with driving force 21°C

Exp. No.	System	Experimental Pressure [MPa]	ΔT^a [°C]	Dissociation Temperature, T_d^b [°C]	CH_4 Released [mol/mol of H_2O]	CH_4 Recovery [mol%]
7	$HS/H_2O/CH_4$	6.5	21	8.1	0.1411	88.87
8	$HS/H_2O/CH_4$	6.5	21	8.4	0.1388	82.55
9	$HS/H_2O/CH_4$	6.5	21	8.1	0.1370	90.16
				Average	0.1390±0.0021	87.19±4.07
10	$HS/H_2O/CH_4$	5	21	5.9	0.1326	90.16
11	$HS/H_2O/CH_4$	5	21	6.2	0.1325	93.29
12	$HS/H_2O/CH_4$	5	21	5.8	0.1442	91.37
				Average	0.1364±0.0068	91.61±1.58

$^a\Delta T = T_{end} - T_{start}$

^bT_d = Dissociation temperature

Figure 4.12 shows the methane released and temperature profiles in the system of $HS/H_2O/CH_4$ at 6.5 MPa and 21°C temperature driving force. As seen from the figure, the thermocouple T1 takes the longest time for dissociation, which means the methane hydrate formed at location T1 is more stable than the hydrate formed in other locations. After the methane hydrate dissociation is completed, the temperatures gradually increase in the same trend with the temperature of water until it reaches the plateau at the desired temperature (25°C).

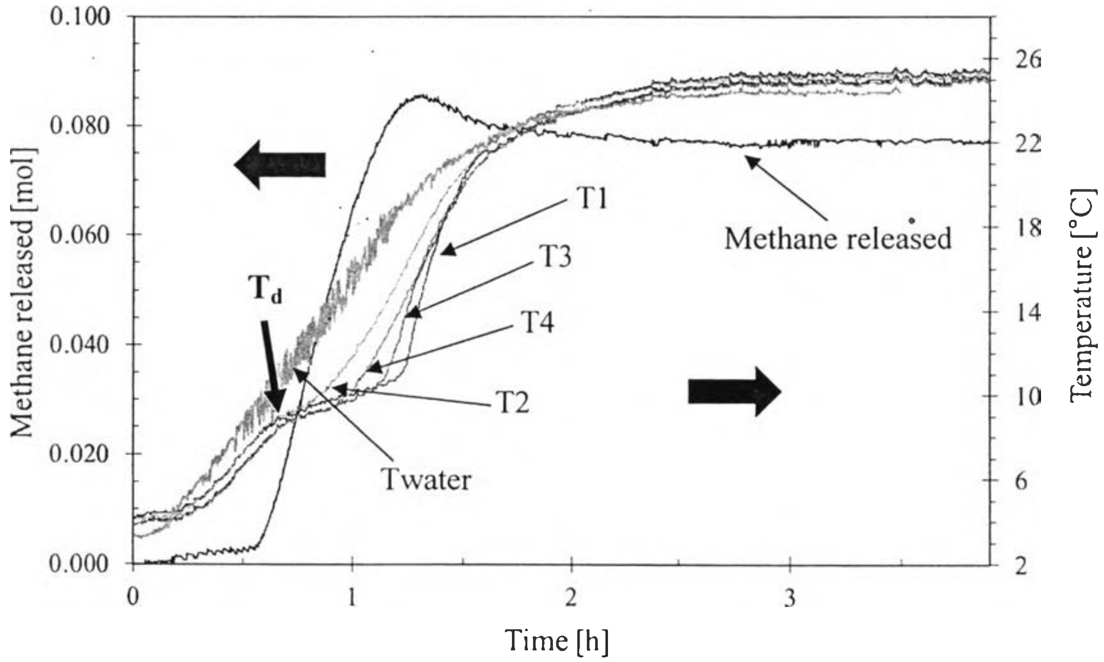

Figure 4.12 Methane released and temperature profiles in the system of $HS/H_2O/CH_4$ at 6.5 MPa and temperature driving force = 21°C (Experiment 8, Table 4.4).

Methane released and temperature profiles in the system with hollow silica at experimental pressure of 5 MPa (temperature driving force = 21°C) is shown in Figure 4.13. Methane released and temperature profiles in the system at 5 MPa are similar to 6.5 MPa.

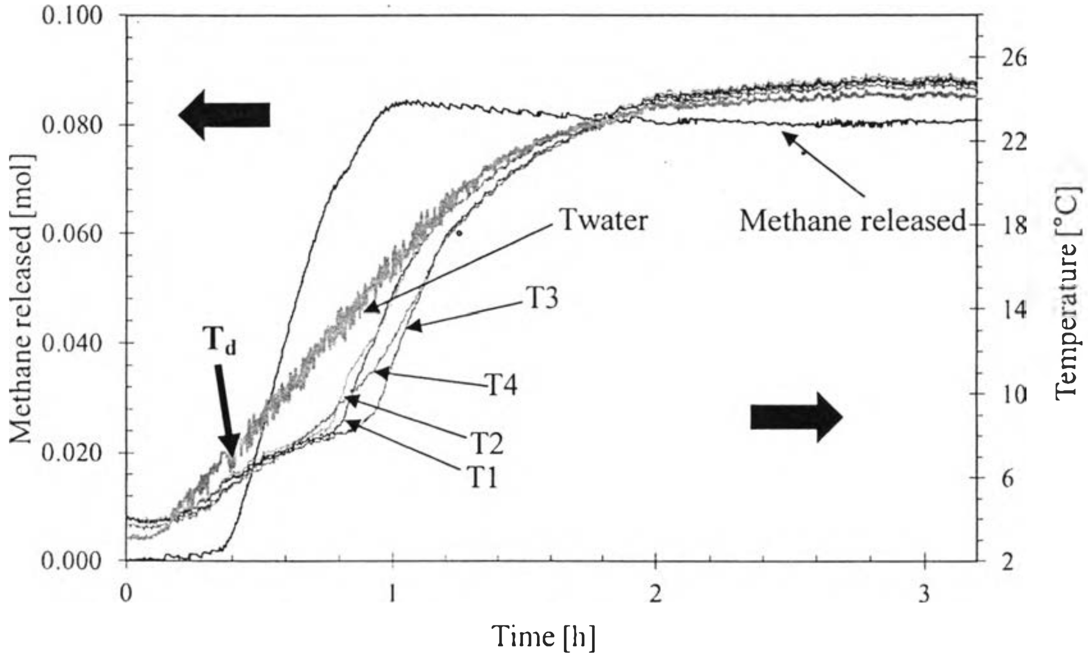

Figure 4.13 Methane released and temperature profiles in the system of the HS/H_2O/CH_4 at experimental pressure of 5 MPa and temperature driving force = 21°C (Experiment 12, Table 4.4).

Comparison of the methane released during the methane hydrate dissociation in the system of HS/H_2O/CH_4 at 6.5 MPa and 5 MPa and 4°C is presented in Figure 4.14. The methane gas in the system at 5 MPa starts releasing from the methane hydrate faster than that at 6.5 MPa. However, the rate of methane hydrate dissociation and the amount of methane released are almost the same in both conditions. From Figure 4.14, the methane gas released is increased rapidly before slightly decreasing and reaching the plataue. A reason is, after reaching the T_d, the pressure is increased rapidly because the methane gas is released from the hydrate crystal. When the methane gas reaches maximum gas released, the system tries to adjust to reach the equilibrium at that temperature by decreasing the pressure of the system so some of methane gas may adsorb on the hollow silica bed again.

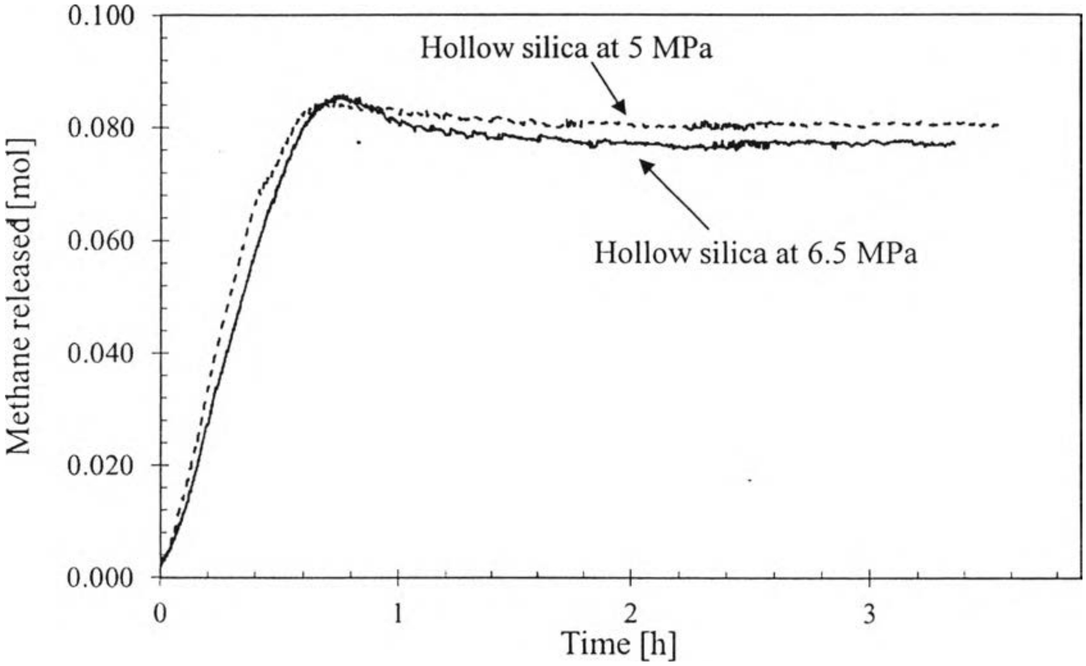

Figure 4.14 Comparison of the methane released during the methane hydrate dissociation in the system of $HS/H_2O/CH_4$ at 6.5 MPa and 5 MPa and temperature driving force = 21°C (Experiments 2 and 6, respectively, Table 4.4). Time zero in the figure corresponds to the first point of hydrate released.

4.3 Comparison of the Effects of Hollow Silica and Activated Carbon

4.3.1 Methane Hydrate Formation

The methane gas uptakes in the systems of $HS/H_2O/CH_4$ and $AC/H_2O/CH_4$ are compared in Figure 4.15. The rate of methane hydrate formation in the system of $HS/H_2O/CH_4$ is significantly higher than the activated carbon system at both experimental pressures. The different of experimental pressure affects the amount of gas uptake and the rate of methane hydrate formation in the system with the presence of activated carbon but not in the system with hollow silica. However, the formation time for first hydrate formation is influenced by the pressure in both porous media systems. The formation time of the methane hydrate formation at 8 MPa is shorter than the system at 6 MPa in both porous media.

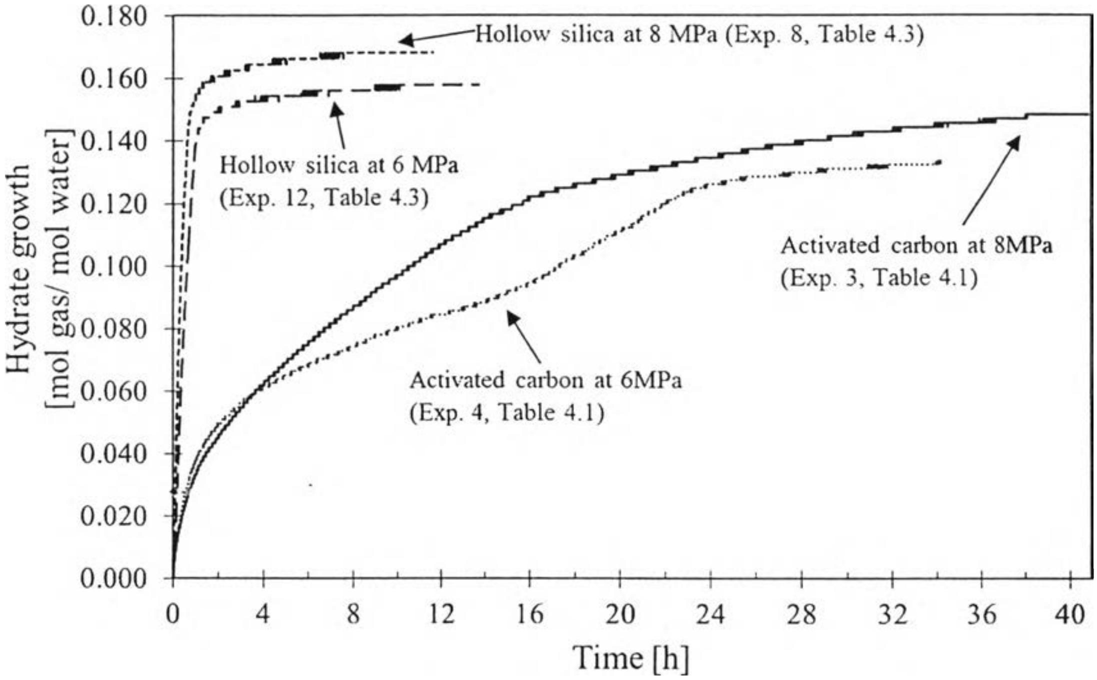

Figure 4.15 Comparison of gas uptake during the methane hydrate formation in the systems of HS/H_2O/CH_4 and AC/H_2O/CH_4 at 8 MPa and 6 MPa. Time zero in the figure corresponds to the first point of hydrate growth.

Although the methane consumption in the system of HS/H_2O/CH_4 is almost the same as the system of AC/H_2O/CH_4 at 8 MPa, the methane consumption of the hollow silica is significantly higher than the latter at 6 MPa. Furthermore, the amount of methane consumed in the system of HS/H_2O/CH_4 at 6 MPa is close to the system of AC/H_2O/CH_4 at 8 MPa. The rate of gas uptake of hollow silica system at 6 MPa is faster than the activated carbon system at 8 MPa. Therefore, the methane hydrate formation with the presence of hollow silica is effective at lower pressure than the system with activated carbon.

Although the activated carbon has higher surface area than the hollow silica (907.1 m^2/g compared to 1.3 m^2/g), the different in the pore structures of activated carbon may obstruct the diffusion of gas into water, and methane hydrate may form at the surface of activated carbon, resulting in the slow of methane hydrate formation of the system with activated carbon compared to hollow silica (Kang and Lee., 2010). The hollow silica can adsorb water molecules into ordered layers due to the hydrophilic surface, indicated by silanol group (Si-O-H) (Cha *et al.*, 1988, Prasad *et al.*, 2014). This is why the hydrate crystal is formed easily in hollow silica. Moreover, a very low density of hollow silica causes the methane gas to flow through hollow silica easier than activated carbon. The hollow silica particles, saturated by water molecules may disperse when methane gas is introduced in the system. The dispersed particles increase the interface area between gas molecules and water molecules, so the mass transfer of gas into water to form methane hydrate is increased.

4.3.2 Methane Hydrate Dissociation

Comparison of the methane released during the methane hydrate dissociation in the systems of HS/H_2O/CH_4 and AC/H_2O/CH_4 at 6.5 MPa and 5 MPa with 21°C driving force is shown in Figure 4.16. The final amount of methane released in all conditions is not significantly changed. Thus, the experimental pressure in the dissociation experiments does not affect to the systems of HS/H_2O/CH_4 and AC/H_2O/CH_4 at the same temperature driving force. The methane hydrate dissociation rate in the system of HS/H_2O/CH_4 is faster than that of AC/H_2O/CH_4. Chari *et al.* (2013) reported that the different sizes of porous media particles influenced the methane hydrate dissociation rate. The smaller particles showed higher dissociation rate than the larger particles. Moreover, the methane gas can be released through the small particles of hollow silica easier than the bed of activated carbon, so the dissociation rate in the system with hollow silica is higher. As mentioned before, the phenomena that methane hydrate is slightly decreased before it reaches plateau can be observed in the system of HS/H_2O/CH_4, whereas it is not found in the system of AC/ H_2O/CH_4 because the pores of activated carbon may obstruct the rate of methane released so the methane gas was gradually releases and the system can adjust the equilibrium along with the methane released. Thus, the slightly decreasing before reaches equilibrium is not found in the activated carbon system.

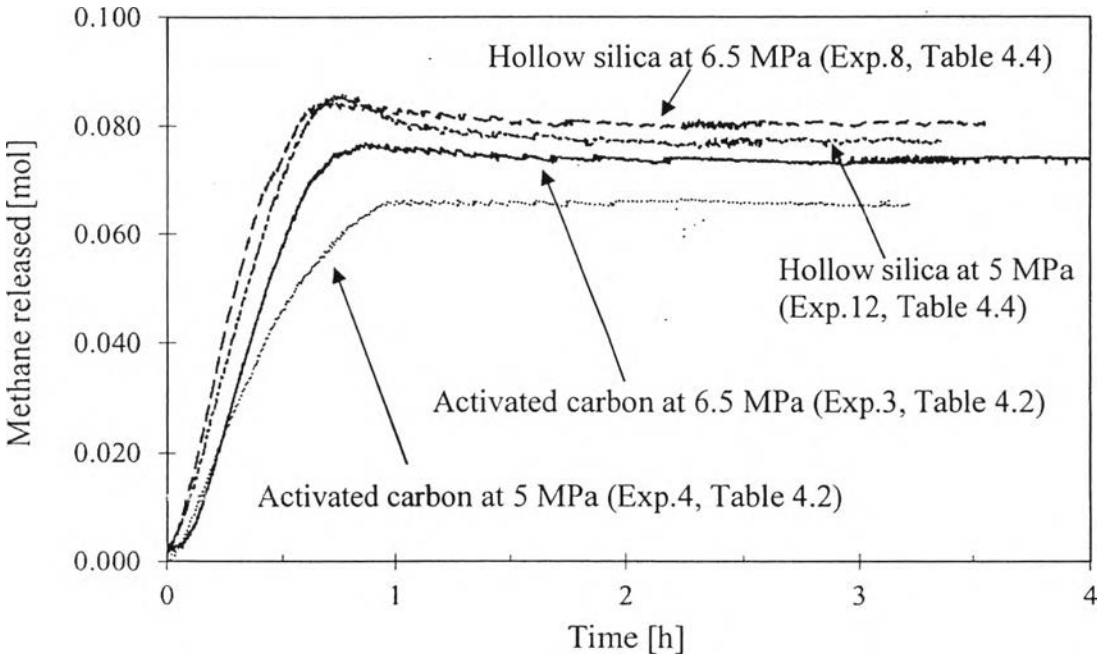

Figure 4.16 Comparison of the methane released during the methane hydrate dissociation in the system of the HS/H_2O/CH_4 and AC/H_2O/CH_4 at 6.5 MPa and 5 MPa (temperature driving force = 21°C). Time zero in the figured corresponds to the first point of hydrate released.

The hydrate phase equilibrium point is also observed in this study. The different experimental pressure in the methane hydrate dissociation shows the different dissociation temperature that can be used to plot the hydrate phase equilibrium points, as shown in Figure 4.17. Kang *et al.* (2010) and Sun *et al.* (2014) discovered the shifting of hydrate phase equilibrium. They reported that the hydrate phase equilibrium is affected by the capillary force between particles and water activity. The pore capillary force of smaller grain is greater than larger grain so the formation of hydrates in the fined grain is harder. Moreover, the attraction of particles surface reduces activity of free water that decreases the free water to form hydrates. Thus, the equilibrium curve of smaller grain is shifted to a higher pressure and a lower temperature that means hydrate regions is decreased from the bulk system. However, the hydrate phase equilibrium points in the systems of HS/H_2O/CH_4 and AC/H_2O/CH_4 are not significantly different from the pure water system, reported by Zanota *et al.* (2005). Similar to Siangsai *et al.*, (2012), the porous media does not significantly change the thermodynamic of methane hydrate. In other words, the porous media in the methane hydrate system does not affect to hydrate phase equilibrium.

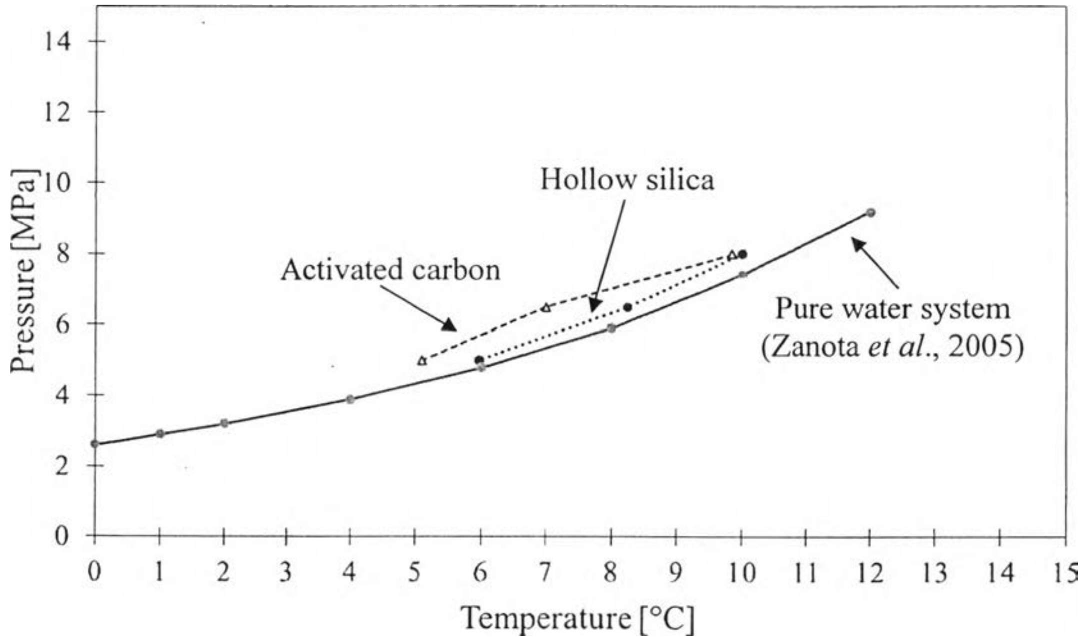

Figure 4.17 Methane hydrate phase equilibrium points of methane hydrate of the HS/H_2O/CH_4 and AC/H_2O/CH_4 and pure water system.